

In vitro evolution of single-chain antibodies using mRNA display

Isao Fukuda, Kanehisa Kojoh, Noriko Tabata, Nobuhide Doi, Hideaki Takashima, Etsuko Miyamoto-Sato and Hiroshi Yanagawa*

Department of Biosciences and Informatics, Keio University, 3-14-1 Hiyoshi, Kohoku-ku, Yokohama 223-8522, Japan

Received June 19, 2006; Revised August 4, 2006; Accepted August 5, 2006

ABSTRACT

Here we describe the application of the *in vitro* virus mRNA display method, which involves covalent linkage of an *in vitro*-synthesized antibody (phenotype) to its encoding mRNA (genotype) through puromycin, for *in vitro* evolution of single-chain Fv (scFv) antibody fragments. To establish the validity of this approach to directed antibody evolution, we used random mutagenesis by error-prone DNA shuffling and off-rate selection to improve the affinity of an anti-fluorescein scFv as a model system. After four rounds of selection of the library of mRNA-displayed scFv mutants, we obtained six different sequences encoding affinity-matured mutants with five consensus mutations. Kinetic analysis of the mutant scFvs revealed that the off-rates have been decreased by more than one order of magnitude and the dissociation constants were improved ~30-fold. The antigen-specificity was not improved by affinity maturation, but remained similar to that of the wild type. Although the five consensus mutations of the high-affinity mutants were scattered over the scFv sequence, analysis by site-directed mutagenesis demonstrated that the critical mutations for improving affinity were the two that lay within the complementarity determining regions (CDRs). Thus, mRNA display is expected to be useful for rapid artificial evolution of high-affinity diagnostic and therapeutic antibodies by optimizing their CDRs.

INTRODUCTION

Selection technologies, to obtain monoclonal antibodies with high affinity and specificity against defined antigens, are required for the development of diagnostic and therapeutic antibodies [reviewed in (1–4)], both to improve the detection limit for diagnostics and to decrease the required dose for therapeutics. In immunized animals, affinity maturation of

antibodies occurs via repeated stimulation of antigen-specific proliferation of B cells and accumulation of point mutations introduced into the DNA (5–7). Therefore, it has been suggested that the affinity of antibodies can be improved by mimicking affinity maturation in the laboratory (8,9). For the *in vitro* evolution of recombinant antibodies such as single-chain Fv (scFv) and Fab antibodies, several display technologies such as phage display (10), yeast surface display (11), ribosome display (12–15) and DNA display (16) have been used to link an antibody (phenotype) and its encoding nucleic acid (genotype).

In this study, we have applied our *in vitro* virus (IVV) mRNA display system (17–19) for directed evolution of a single-chain antibody for the first time, although evolution of antibody mimics (fibronectin type III domains) using mRNA display has been reported previously (20,21). In mRNA display, an *in vitro*-synthesized polypeptide is covalently attached to its encoding mRNA through puromycin (17,19,22). Unlike phage display and yeast surface display, mRNA display (as well as ribosome display) is a totally *in vitro* system that does not require the transformation of living cells; thus, very large protein libraries (>10¹⁰ unique members) can easily be constructed and used for the selection of antibodies directed against antigens of interest. The covalent bond of the mRNA–protein complex in mRNA display should be more stable than the protein–ribosome–mRNA complex used in ribosome display with respect to thermal or physicochemical stress as a selection pressure. For the present study, we used an anti-fluorescein antibody as a model, because it has been well-characterized both structurally and kinetically (23,24). Further, laboratory evolution of the anti-fluorescein antibody was previously performed by yeast surface display (11) and ribosome display (14); hence, the antibody is a suitable model for evaluating our new method in comparison with the previous methods.

MATERIALS AND METHODS

DNA preparation

The oligonucleotide sequences used in this study are listed in Table 1. A DNA fragment that contains an SP6 promoter, the

*To whom correspondence should be addressed. Tel: +81 45 566 1775; Fax: +81 45 566 1440; Email: hyana@bio.keio.ac.jp

0.22 μm Ultrafree-MC filter (Millipore) and purified with the RNeasy mini kit. The purified mRNA was reverse-transcribed with ReverTra Ace reverse-transcriptase (Toyobo) using a FlaA-R primer for 1 h at 42°C. Subsequently, the RT product was directly amplified by PCR with KOD-plus DNA polymerase using W29ATG-F and FlaA-R primers (24 cycles at 96°C for 30 s; at 58°C for 30 s; and at 72°C for 1 min). The PCR product was purified using a QIAquick PCR purification kit (Qiagen).

Cloning and sequencing

The selected DNAs after four rounds were cloned using a TOPO TA cloning kit (Invitrogen) and sequenced with the ABI PRISM 3100 genetic analyzer. Subsequently, a signal sequence (pelB) for periplasmic secretion was added to each scFv gene by overlap extension PCR with KOD-plus DNA polymerase using 0.4 μM primers pelB-F and Flag-R and a 0.02 μM primer pelBleader-F (15 cycles at 96°C for 30 s; at 58°C for 30 s; and at 72°C for 1 min). The PCR products were purified using the QIAquick PCR purification kit and subcloned using a Champion pET directional TOPO expression kit (Invitrogen).

Overexpression and purification

The BL21star(DE3)pLysS cells harboring the vector pET101/D-TOPO for the expression of scFv mutants with a C-terminal hexahistidine tag were grown in 1.5 liters of TB medium containing 100 $\mu\text{g}/\text{ml}$ ampicillin at 30°C. When the culture attained an optical density of 0.8 at 600 nm, the cells were induced by the addition of isopropylthio- β -D-galactoside (final 1 mM). After an additional 3 h incubation, the cells were harvested by centrifugation and resuspended in 15 ml/g cell of osmotic buffer (30 mM Tris-HCl, pH 7.6, 1 mM EDTA and 0.5 mM sucrose). Again, the cells were harvested by centrifugation and resuspended in 5 ml/g cell of ice-cold Milli-Q water. The centrifuged supernatant was recovered and further centrifuged for 20 min at 15 000 g to separate an insoluble fraction. The supernatant was recovered as the periplasmic extract for competitive ELISA analysis. The protein concentration was evaluated by SDS-PAGE and Western blot analysis using HRP-conjugated anti-FLAG M2 antibody (Sigma).

For purification of proteins, the cells were grown as described above, harvested by centrifugation, and resuspended in 30 ml of TBS containing 100 U of DNase I (Promega), the EDTA-free protease inhibitor cocktail (Nacalai tesque) and 20% glycerol. The cells were lysed by sonication using a Bioruptor UCW-201 (Cosmo Bio) for 50 min at 30 s intervals. The resulting crude extracts were centrifuged for 20 min at 15 000 g and filtered through 0.22 μm PVDF Millex-GV filters (Millipore). The clear solution containing the histidine-tagged scFv protein was purified by immobilized metal affinity chromatography (IMAC) using TALON superflow metal affinity resin (Clontech) on an AKTA-FPLC system (Amersham Biosciences) with running buffer (10 mM HEPES-NaOH, pH 7.4, 150 mM NaCl and 20 mM imidazole) at a flow rate of 0.5 ml/min. The eluate obtained with a step gradient to 80 mM imidazole in running buffer was concentrated in a 30 000 MWCO PES Viva-spin 500 (Viva Science). Subsequently, the monomeric scFv was separated

by size exclusion chromatography using Sephadex G-75 (Amersham Biosciences) with HBS buffer (10 mM HEPES-NaOH, pH 7.4 and 150 mM NaCl) at a flow rate of 0.2 ml/min, and then the buffer was changed to HBS-EP buffer (10 mM HEPES-NaOH, pH 7.4, 150 mM NaCl, 3 mM EDTA and 0.005% Tween-20) by using a MicroSpin G-25 column (Amersham Biosciences). The concentration and purity of scFv were confirmed by BCA assay using a Micro BCA protein assay kit (Pierce) and by CBB staining of SDS-PAGE gel, respectively.

Competitive ELISA

Streptavidin transparent C8 plates (Nunc) were incubated with 1 $\mu\text{g}/\text{ml}$ fluorescein-biotin (Sigma) in 100 μl of blocking solution (Roche) per well for 1 h at 25°C, washed with TBST (TBS, pH 7.4 and 0.2% Tween-20), and blocked with 200 μl of blocking solution per well before use. Separately, the scFv-expressed periplasmic extract or wheat germ cell-free translated product was diluted 5-fold in blocking solution in the presence and absence of free fluorescein (10–1000 nM), and incubated for 1 h at 25°C. Then, the protein solution (100 μl) was transferred into wells on a plate with immobilized antigen and the plate was incubated for 15 min at 25°C. It was immediately washed five times with TBST and further incubated for 1 h with HRP-conjugated anti-FLAG M2 antibody (1:10 000 dilution in TBST; 100 μl per well). The plate was washed five times with TBST and then 100 μl of TMB substrate (Nacalai tesque) was added per well. The reaction was quenched with 1 N H_2SO_4 (100 μl per well) and the absorbance at 450 nm (reference wavelength at 655 nm) was measured. For each clone, the relative binding activity was calculated as the ratio of the ELISA signal in the presence of competitor (fluorescein) to that in the absence of competitor. All the experiments were performed in duplicate.

For the analysis of antigen-specificity, competitive ELISA was performed as described above, except for the use of various concentrations of fluorescein, Oregon green 488 carboxylic acid (Molecular Probes) or rhodamine 110 (Molecular Probes) as the competitor.

Surface plasmon resonance (SPR) spectroscopy

All the experiments were performed in duplicate at 25°C with a Biacore 3000 instrument (Biacore) using HBS-EP buffer. Fluorescein-conjugated BSA (BSA-FITC; Molecular Probes) or BSA (Pierce) as a background control was covalently immobilized onto a CM5 sensor chip (Biacore) by means of the amine coupling procedure according to the standard protocol. To prevent the rebinding of analytes to ligands immobilized on the CM5 sensor chip and to reduce the mass transport limitation effect, the measurements were performed under conditions of low ligand amount (450 resonance units) and high flow rate (60 $\mu\text{l}/\text{min}$). To determine dissociation constants, five different concentrations (8–400 nM) of the purified scFvs were injected. The injection periods for association and dissociation were 1 and 10 min, respectively. The surface of the sensor chip was regenerated by pulse injection of 60 μl of 57 mM HCl (pH 1.2). The binding data were analyzed with the '1:1 binding with mass transfer' model in the BIAevaluation software ver. 4.1 (Biacore).

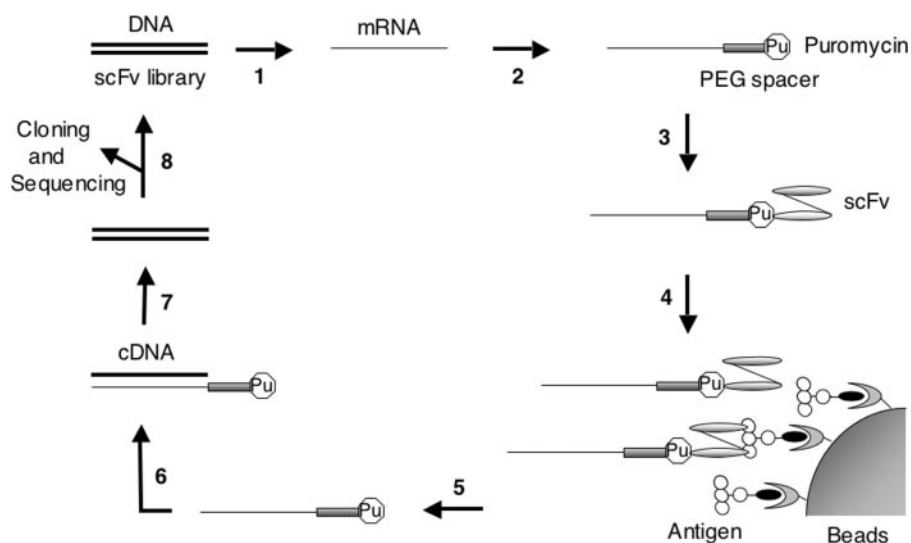


Figure 1. Schematic representation of the *in vitro* selection of scFv antibodies by the IVV method. Step 1: a DNA library of scFv mutants is *in vitro*-transcribed into mRNA. Step 2: the mRNA is enzymatically ligated with puromycin (Pu) through a PEG spacer. Step 3: the ligated product is *in vitro*-translated by a cell-free translation system, resulting in covalent bonding of puromycin with the full-length protein at the C-terminus. Step 4: the mRNA-displayed scFv library is captured on antigen-immobilized beads and unbound molecules are washed away. Step 5: the bound molecules are eluted by protease digestion. Step 6: the mRNA portion of eluted molecules is reverse-transcribed into cDNA. Step 7: the cDNA is amplified by PCR. Step 8: the DNA can be used for the next round of selection after mutagenesis or can be analyzed by cloning and sequencing after several rounds of selection.

RESULTS AND DISCUSSION

Strategy for *in vitro* selection of scFv by mRNA display

The scheme for *in vitro* selection of anti-fluorescein scFv using the IVV method is shown in Figure 1. First we constructed the template DNA for IVV, containing an SP6 promoter and Ω enhancer upstream of the anti-fluorescein scFv gene (V_H -linker- V_L), and the FLAG-tag and poly(A) sequence in the downstream region. The scFv region was subjected to random mutagenesis by error-prone PCR (the error rate was 0.8%; 6–7 nt per scFv gene). The transcribed mRNA (1.2×10^{12}) molecules were attached to a PEG spacer containing puromycin at the 3' end and *in vitro*-translated in 10 μ l of wheat germ cell-free translation system, resulting in the covalent bonding of the C-terminus of the full-length scFv protein (phenotype) with its coding mRNA (genotype) through the puromycin-PEG spacer. We estimated that the number of resultant mRNA-displayed scFv molecules in the initial library was 6×10^{10} (ligation efficiency of mRNA with the puromycin-PEG spacer and efficiency of IVV formation were 50 and 10%, respectively). The library was captured on fluorescein-immobilized beads and the mRNA portion of selected molecules was amplified by RT-PCR. In each round of selection, the recovered DNA was further mutagenized by error-prone DNA shuffling (26,29).

Off-rate selection of the randomized scFv library

We applied off-rate selection (10,14) as a selection pressure for affinity maturation of anti-fluorescein scFv. In off-rate selection, mRNA-displayed scFvs that bound to fluorescein-immobilized beads were washed with a large excess of free fluorescein to prevent the rebinding of antibodies to the beads. Since the off-rate (k_{off}) depends on the half-life ($\tau_{1/2}$) of the antigen-antibody complex, higher-affinity binders with low k_{off} can be retained on the beads for a longer

washing time. We set the time periods of off-rate selection so as to decrease k_{off} about several-fold per round (3, 20, 96 and 336 h). Although mRNA is considered to be a labile molecule, it is stable for at least 2 weeks at low temperature (14).

After four rounds of off-rate selection, the total binding activity of *in vitro*-translated products of the library DNA at each round was analyzed by competitive ELISA. As shown in Figure 2, the binding activity gradually increased in successive rounds of selection (Figure 2; 0 nM), whereas little or no activity was observed in the presence of competitor (Figure 2; 10 nM, 100 nM and 1 μ M), indicating the enrichment of specific binders with high affinity in the library.

Competitive ELISA for the second screening

The library DNA from the fourth round of selection was cloned and sequenced. The rate of amino acid substitutions was 3.5%. Seventy-seven randomly chosen genes were subcloned into an *Escherichia coli* expression vector, their expression was induced, and the binding activity of scFv mutants in the periplasmic extracts was analyzed by ELISA. Clones, whose ELISA signal (OD at 450 nm) was <0.2 , were defined as ELISA-negative and those clones, whose signal was in the range of 0.2–1.0, were defined as ELISA-positive. Out of the 77 clones, 45 clones (58%) were ELISA-positive. In SDS-PAGE analysis, all ELISA-positive clones exhibited protein expression in the periplasm, whereas 27 out of 32 ELISA-negative clones showed little or no expression in the periplasm (data not shown). Although the other five ELISA-negative clones were expressed in periplasm, three of them showed low ELISA signals (<0.2) and two had no binding activity (data not shown).

We estimated the affinity of the 45 ELISA-positive clones by competitive ELISA (Figure 3). The relative binding was

defined as the ratio of the ELISA signal in the presence of free fluorescein as a competitor to that in the absence of the competitor. The lower relative binding of 37 clones than that of wild type indicates that these clones have higher

affinity than the wild type. The six highest-affinity clones with relative binding of <5% and 14 clones with <20% were classed as Group 1 and Group 2, respectively. The amino acid changes are listed in Table 2. All six Group 1 mutants with the highest affinity contain five consensus mutations, W47C in FR H2, D101N in CDR H3, S15F in the linker, V21I in FR L1 and H94Y in CDR L3 (Table 2, boldface), whereas a majority of the 14 Group 2 mutants with moderate affinity contain four consensus mutations, A68V in FR H3, G96D in CDR H3, R18M in FR L1 and H94Y in CDR L3. Notably, the mutation H94Y in CDR L3 was contained in both Group 1 and Group 2 mutants. It is likely that the advantageous mutations were accumulated among the affinity-matured scFv genes during the repetition of DNA shuffling and off-rate selection in the selection cycles.

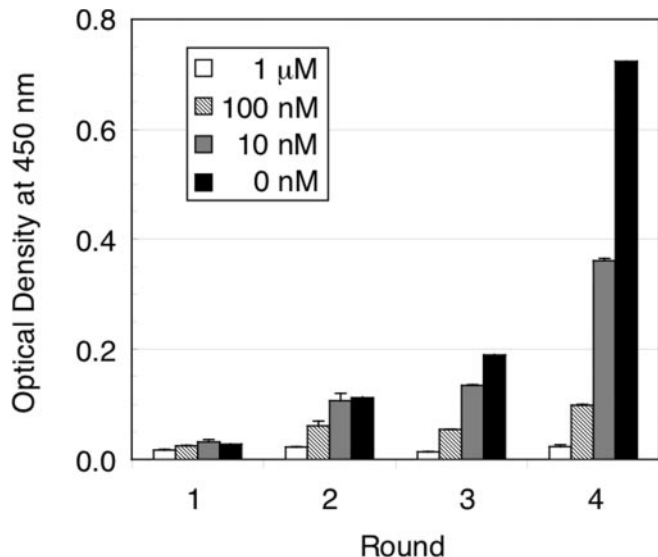


Figure 2. Competitive ELISA for monitoring the fraction of the mutant scFv library that bound to fluorescein at each round of selection. The wheat germ cell-free translated products containing mutant scFv libraries were pre-incubated with a competitor (0–1000 nM free fluorescein) and allowed to bind to fluorescein-immobilized plates. After washing of the plates, remaining scFvs were detected by HRP-conjugated anti-FLAG M2 antibody and TMB substrate with absorbance measurements at 450 nm (reference at 655 nm). All measurements were performed in duplicate.

Characterization of the affinity-matured mutants

The binding affinities of purified scFvs (five Group 1 mutants and a Group 2 mutant, 2-10) were measured by SPR spectroscopy (Table 3 and Figure 4). Although the on-rates of the mutants were similar to that of the wild type, the off-rates were decreased by more than one order of magnitude, suggesting that the application of selection pressure by off-rate selection had been successful. The dissociation constants of Group 1 mutants were improved by ~30-fold, which is comparable with that obtained by ribosome display (14), probably because the selection conditions were similar to each other.

Next, we examined the antigen-specificity of the affinity-matured mutants by competitive ELISA. Two fluorescein analogs, Oregon green 488 and rhodamine green, as well as

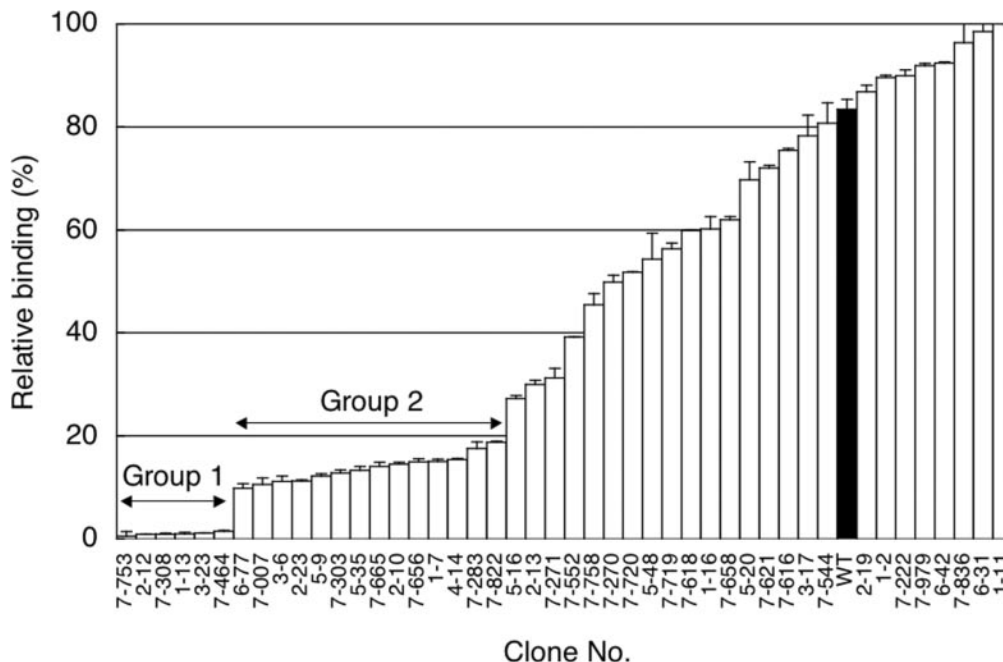


Figure 3. Competitive ELISA for estimating the affinities of 45 selected clones after the fourth round of selection. The periplasmic extracts for wild type and mutant scFv clones were pre-incubated in the presence or absence of 10 nM fluorescein, and then allowed to bind to fluorescein-immobilized plates. After the plates were washed, remaining scFvs were detected by HRP-conjugated anti-FLAG M2 antibody and TMB substrate with absorbance measurements at 450 nm (reference at 655 nm). The relative binding indicates the ratio of the ELISA signal in the presence of the competitor to that in the absence of the competitor; thus, lower relative binding of clones compared with the wild-type scFv (WT; filled bar) indicates that these clones have higher affinity than the wild type. All the measurements were performed in duplicate.

Table 2. Mutations in scFv fragments selected by the IVV method

Clone	V _H	V _L	Linker
Group 1			
7-753	W47C, D101N	V21I, S76T, H94Y	S15F
2-12	W47C, A68T, K73Q, D101N	V21I, H94Y	S15F
7-308	W47C, D101N	V21I, A51V, H94Y	S15F
1-13	K19R, S21T, W47C, S74N, S76G, S82bG, E85D, D101N, Y102N, S112F	V21I, S80T, H94Y, E105K	G12S, S15F
3-23	K19R, W47C, S74N, Q81H, S82bG, D101N, Y102N	V21I, S80T, H94Y	G12S, S15F
7-464	W47C, K62N, K73I, D101N	V21I, Q38H, H94Y	S15F
Group 2			
6-77	G96D	M11L, P59S, H94Y	G19D
7-007	A68V, G96D, S112P	R18M, H94Y	
3-6	A68V, G96D	R18M, H94Y	S5L
2-23	A68V, G96D	R18M, Y53H, H94Y	
5-9	A68V, Q81R, D101N	V21I, D30H	S15F
7-303	A68V, G96D	T13I, R18M, D70S, H94Y, L104M	
5-35	A68V, G96D	R18M, P59H, S67Y, H94Y	
7-665	A68V, G96D	R18M, K24R, L83S, H94Y	S20I
2-10	A68V, G96D	R18M, H94Y	
7-656	S30T, M80L, Y99H	T22I, A84T, H94Y, K103M	S15P
1-7	N58I, G96D	I2V, V21I, N32K, Y53C, D60G	
4-14	Q3R, W47C, S76R, M80L, Y99N	H94Y	
7-283	W47C, S76R, M80L, Y99N	G68R, H94Y	
7-822	K64N, A68V, G96D	R18M, H94Y	G11C

Amino acid mutations of the V_H, V_L and linker regions of selected mutants. Residue numbering is according to Kabat *et al.* (32). The original sequence of the wild type is shown in (14). Group 1 and Group 2 indicate 6 clones with high activity and 14 clones with moderate activity, respectively (see also Figure 3). Boldface residues indicate five consensus mutations.

Table 3. Kinetic parameters of selected clones

Clone	k_{on} ($M^{-1} s^{-1} \times 10^5$)	k_{off} ($s^{-1} \times 10^{-4}$)	K_D (nM)	$\tau_{1/2}$ (min)
Wild type	$1.0 \pm 0.05^*$	33 ± 0.62	32	3.5
2-12	1.9 ± 0.02	1.8 ± 0.007	0.95	64
3-23	3.7 ± 0.06	3.3 ± 0.17	0.88	35
7-308	3.6 ± 0.02	3.6 ± 0.01	0.99	33
7-464	1.2 ± 0.002	1.7 ± 0.009	1.4	70
7-753	1.1 ± 0.02	1.8 ± 0.008	1.7	63
2-10	0.26 ± 0.002	2.0 ± 0.18	7.5	59

*Mean \pm SEM.

fluorescein were used as competitors (Figure 5A). The affinity of Group 1 mutant 2-12 (Figure 5C) was higher than that of wild type (Figure 5B), not only for fluorescein but also for the two fluorescein analogs, with an almost identical ratios of increase. Similar results were obtained for the other five Group 1 mutants (data not shown). The results suggest that the specificity of the affinity-matured mutants was not altered, but remained similar to that of the wild type.

To determine the most important mutations for affinity improvement, we first constructed an scFv mutant that contains only the five consensus mutations in Group 1 mutants (named CM5). As shown in Figure 6A (filled triangles), the activity of the CM5 mutant was similar to that of Group 1 mutants (such as 2-12 shown in Figure 5C, filled squares), indicating that only the five mutations in Group 1 contribute significantly to the increased affinity. Subsequently, we constructed and examined five scFv mutants, each with a single amino acid mutation, W47C, D101N, S15F, V21I or H94Y. Three mutations, W47C and V21I in the framework and S15F in the linker, did not influence binding activity (Figure 6B), whereas two, D101N or H94Y in the CDR, resulted in intermediate binding activity between CM5 and wild type (Figure 6C). Moreover, the double mutant

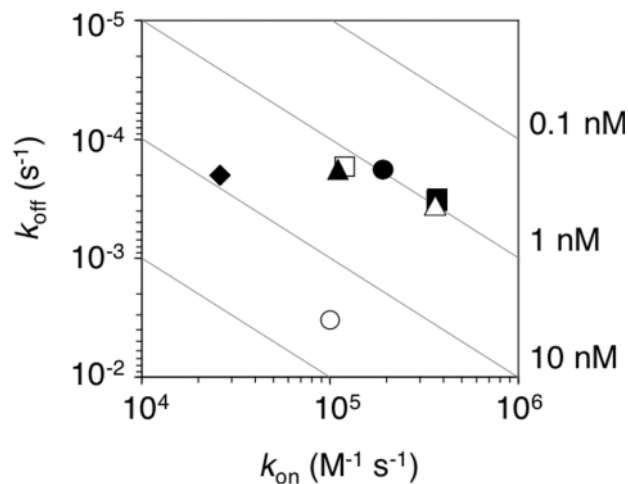


Figure 4. Kinetic distribution plot. The kinetic parameters of purified scFvs were determined by SPR spectroscopy (see Materials and Methods and Table 3). The wild type (open circle); Group 1 mutants 2-12 (filled circle), 7-753 (open square), 3-23 (filled square), 7-308 (open triangle) and 7-464 (filled triangle); and Group 2 mutant 2-10 (filled diamond). The dissociation constants ($K_d = k_{off}/k_{on}$) are represented as gray lines (0.1–10 nM). Group 1 mutants with highest affinity were clustered in the upper right-hand corner of the plot.

containing both D101N and H94Y showed binding activity similar to that of CM5 (Figure 6C, filled diamonds). These results clearly demonstrated that the critical mutations for improving affinity are D101N and H94Y in CDR3 of V_H and V_L, respectively. This result is consistent with the previous findings in laboratory evolution of high-affinity scFv mutants with CDR mutations (11,14). The locations of the CDR mutations on the three-dimensional structure were very close to the fluorescein site (14). It has been argued that the mutation H94Y in V_L directly affects the interaction

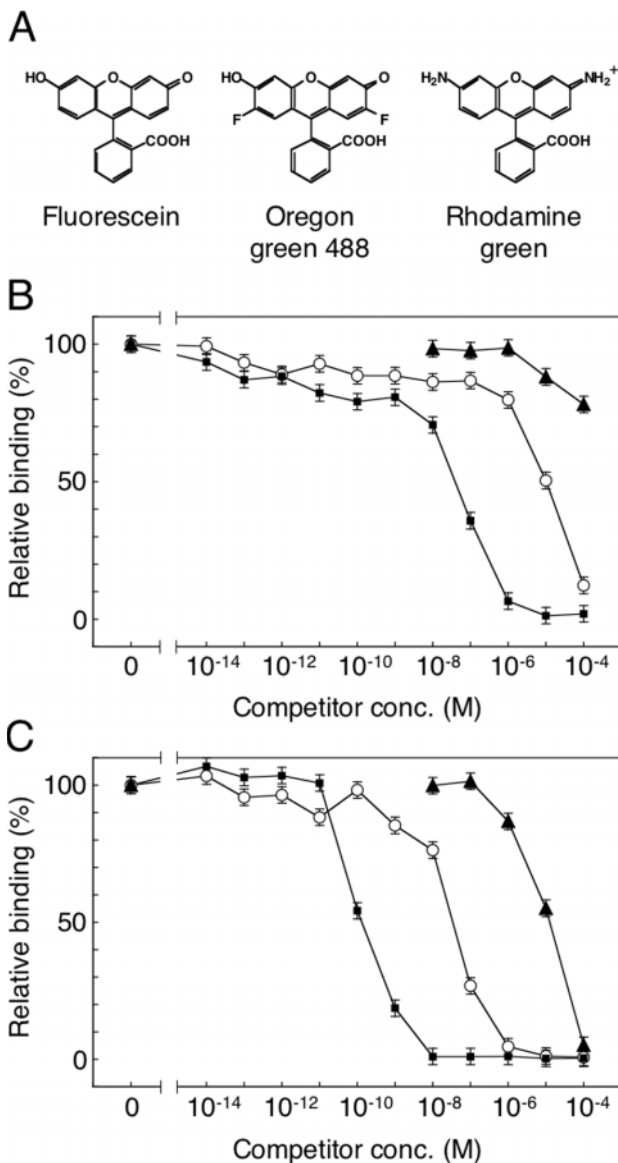


Figure 5. Competitive ELISA for estimating the antigen-specificity of the affinity-matured mutants. (A) The structures of fluorescein, Oregon green 488 and rhodamine green. For immobilization on the ELISA plates, biotin is attached to the benzene moiety of fluorescein; thus, differences of the xanthene moiety would be critical for scFv binding. The periplasmic extracts of the wild type (B) and a typical mutant 2-12 (C) were pre-incubated in the presence of various concentrations of fluorescein (filled squares), Oregon green 488 (open circles) or rhodamine green (filled triangles). The other five mutants in Group 1 gave similar curves. For experimental details, see the legend of Figure 3 and Materials and Methods.

with the antigen in the antigen-binding site, and that mutations D101G, D101A and D101S in V_H break the salt bridge between D101 and R94 in V_H and increase the flexibility of CDR H3 (14). Our results suggest that the mutation D101N in V_H also affects the affinity via a mechanism similar to that of the mutations D101G, D101A and D101S. The framework mutations W47C in V_H and V21I in V_L , as well as the linker mutation S15F, may be neutral mutations fixed in an early round of selection by random genetic drift.

In summary, completely *in vitro* evolution of a single-chain antibody by using the IVV mRNA display method

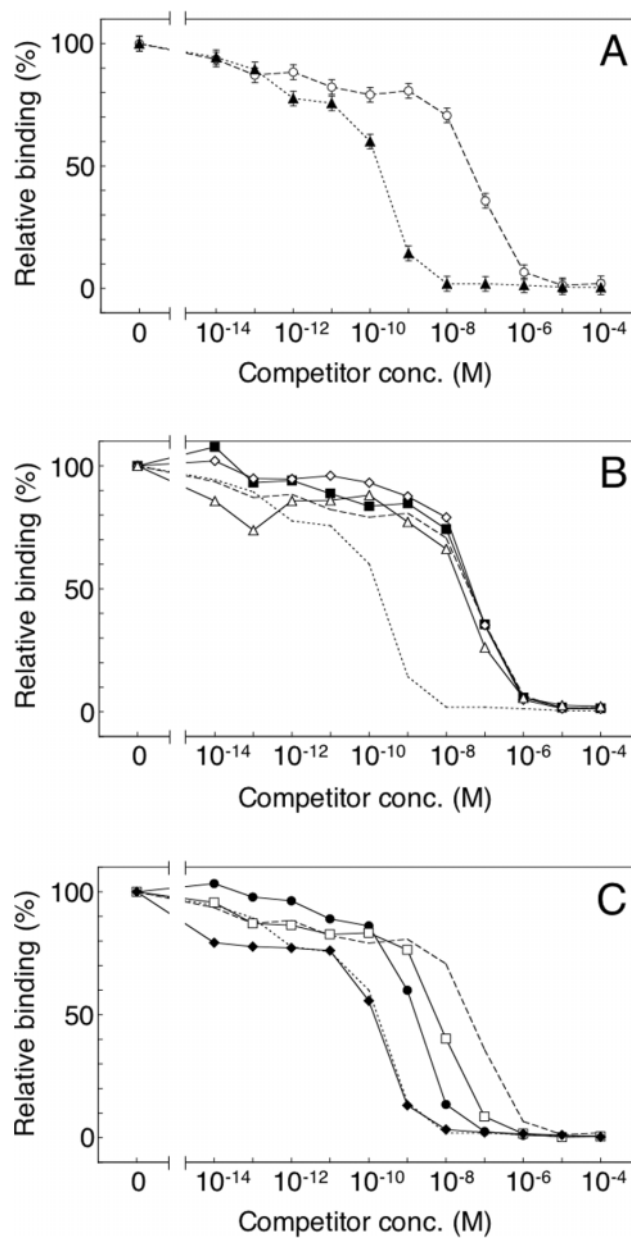


Figure 6. Competitive ELISA for analysis of the contributions of the five consensus mutations in Group 1 mutants. The periplasmic extracts of the wild-type and mutant scFvs were pre-incubated in the presence of various concentrations of fluorescein. For experimental details, see the legend of Figure 3 and Materials and Methods. (A) The wild type (open circles, dashed line) and the mutant CM5 (filled triangles, dotted line). (B) The single mutants W47C (filled squares), V21I (open diamonds) and S15F (open triangles); the wild type (a dashed line) and CM5 (a dotted line). (C) The single mutants D101N (filled circles) and H94Y (open squares); the double mutant D101N/H94Y (filled diamonds); the wild type (dashed line) and CM5 (dotted line).

was accomplished for the first time. By means of the combination of off-rate selection and DNA shuffling, the affinity of scFv mutants was improved ~30-fold without affecting the specificity. The critical mutations D101N in V_H and H94Y in V_L located within the CDRs are similar to those previously found by ribosome display (14). Although both mRNA display and ribosome display are totally *in vitro* selection systems that allow the selection of antibodies against novel

antigens, including toxic molecules, from a huge library, only fewer applications of mRNA display than that of ribosome display have been reported so far (30). Our results demonstrate that mRNA display can be expected to be useful for rapid and efficient evolution of high-affinity antibodies for diagnostic and therapeutic applications by optimizing the CDRs. Furthermore, in comparison with ribosome display, the use of a covalent bond in mRNA display should allow *in vitro* selection of antibodies with high stability at a higher temperature or in the presence of denaturants of ribosomes, as well as the selection of metal-dependent antibodies (31) in the presence and absence of EDTA. We believe that this method should also be applicable to *in vitro* selection of scFv antibodies directed against various antigens from naive or synthetic scFv libraries.

ACKNOWLEDGEMENTS

The authors thank Nobutaka Matsumura, Michiko Onimaru, Toru Tsuji, Masamichi Ishizaka, Seiji Tateyama and Kenichi Horisawa for experimental advice and useful discussions. This research was supported in part by the Industrial Technology Research Grant Program in 2005 from the NEDO of Japan, and by a Grant-in-Aid for Scientific Research and a Special Coordination Fund grant from the MEXT of Japan. Funding to pay the Open Access publication charges for this article was provided by Keio University.

Conflict of interest statement. None declared.

REFERENCES

1. Hoogenboom, H.R. (2005) Selecting and screening recombinant antibody libraries. *Nat. Biotechnol.*, **23**, 1105–1116.
2. Holliger, P. and Hudson, P.J. (2005) Engineered antibody fragments and the rise of single domains. *Nat. Biotechnol.*, **23**, 1126–1136.
3. Wu, A.M. and Senter, P.D. (2005) Arming antibodies: prospects and challenges for immunoconjugates. *Nat. Biotechnol.*, **23**, 1137–1146.
4. Adams, G.P. and Weiner, L.M. (2005) Monoclonal antibody therapy of cancer. *Nat. Biotechnol.*, **23**, 1147–1157.
5. French, D.L., Laskov, R. and Scharff, M.D. (1989) The role of somatic hypermutation in the generation of antibody diversity. *Science*, **244**, 1152–1157.
6. Nossal, G.J.V. (1992) The molecular and cellular basis of affinity maturation in the antibody response. *Cell*, **68**, 1–2.
7. Berek, C. (1993) Somatic mutation and memory. *Curr. Opin. Immunol.*, **5**, 218–222.
8. Marks, J.D., Hoogenboom, H.R., Griffiths, A.D. and Winter, G. (1992) Molecular evolution of proteins on filamentous phage: mimicking the strategy of the immune system. *J. Biol. Chem.*, **267**, 16007–16010.
9. Irving, R.A., Coia, G., Roberts, A., Nuttall, S.D. and Hudson, P.J. (2001) Ribosome display and affinity maturation: from antibodies to single V-domains and steps towards cancer therapeutics. *J. Immunol. Methods*, **248**, 31–45.
10. Hawkins, R.E., Russell, S.J. and Winter, G. (1992) Selection of phage antibodies by binding affinity: mimicking affinity maturation. *J. Mol. Biol.*, **226**, 889–896.
11. Boder, E.T., Midelfort, K.S. and Wittrup, K.D. (2000) Directed evolution of antibody fragments with monovalent femtomolar antigen-binding affinity. *Proc. Natl Acad. Sci. USA*, **97**, 10701–10705.
12. Hanes, J. and Plückthun, A. (1997) *In vitro* selection and evolution of functional proteins by using ribosome display. *Proc. Natl Acad. Sci. USA*, **94**, 4937–4942.
13. He, M. and Taussig, M.J. (1997) Antibody–ribosome–mRNA (ARM) complexes as efficient selection particles for *in vitro* display and evolution of antibody combining sites. *Nucleic Acids Res.*, **25**, 5132–5134.
14. Jermutus, L., Honegger, A., Schwesinger, F., Hanes, J. and Plückthun, A. (2001) Tailoring *in vitro* evolution for protein affinity and stability. *Proc. Natl Acad. Sci. USA*, **98**, 75–80.
15. Zahnd, C., Spinelli, S., Luginbuhl, B., Amstutz, P., Cambillau, C. and Plückthun, A. (2004) Directed *in vitro* evolution and crystallographic analysis of a peptide-binding single chain antibody fragment (scFv) with low picomolar affinity. *J. Biol. Chem.*, **279**, 18870–18877.
16. Reiersen, H., Løbersli, I., Løset, G.Å., Hvattum, E., Simonsen, B., Stacy, J.E., McGregor, D., Fitzgerald, K., Welschof, M., Brekke, O.H. *et al.* (2005) Covalent antibody display: an *in vitro* antibody-DNA library selection system. *Nucleic Acids Res.*, **33**, e10.
17. Nemoto, N., Miyamoto-Sato, E., Husimi, Y. and Yanagawa, H. (1997) *In vitro* virus: bonding of mRNA bearing puromycin at the 3'-terminal end to the C-terminal end of its encoded protein on the ribosome *in vitro*. *FEBS Lett.*, **414**, 405–408.
18. Miyamoto-Sato, E., Nemoto, N., Kobayashi, K. and Yanagawa, H. (2000) Specific bonding of puromycin to full-length protein at the carboxyl terminus. *Nucleic Acids Res.*, **28**, 1176–1182.
19. Miyamoto-Sato, E., Takashima, H., Fuse, S., Sue, K., Ishizaka, M., Tateyama, S., Horisawa, K., Sawasaki, T., Endo, Y. and Yanagawa, H. (2003) Highly stable and efficient mRNA templates for mRNA–protein fusions and C-terminally labeled proteins. *Nucleic Acids Res.*, **31**, e78.
20. Xu, L., Aha, P., Gu, K., Kuimelis, R.G., Kurz, M., Lam, T., Lim, A.C., Liu, H., Lohse, P.A., Sun, L. *et al.* (2002) Directed evolution of high-affinity antibody mimics using mRNA display. *Chem. Biol.*, **8**, 933–942.
21. Parker, M.H., Chen, Y., Danehy, F., Dufu, K., Ekstrom, J., Getmanova, E., Gokemeijer, J., Xu, L. and Lipovsek, D. (2005) Antibody mimics based on human fibronectin type three domain engineered for thermostability and high-affinity binding to vascular endothelial growth factor receptor two. *Protein Eng. Des. Sel.*, **9**, 435–444.
22. Roberts, R.W. and Szostak, J.W. (1997) RNA–peptide fusions for the *in vitro* selection of peptides and proteins. *Proc. Natl Acad. Sci. USA*, **94**, 12297–12302.
23. Whitlow, M., Howard, A.J., Wood, J.F., Voss, E.W., Jr and Hardman, K.D. (1995) 1.85 Å structure of anti-fluorescein 4-4-20 Fab. *Protein Eng.*, **8**, 749–761.
24. Schwesinger, F., Ros, R., Strunz, T., Anselmetti, D., Güntherodt, H.-J., Honegger, A., Jermutus, L., Tiefenauer, L. and Plückthun, A. (2000) Unbinding forces of single antibody–antigen complexes correlate with their thermal dissociation rates. *Proc. Natl Acad. Sci. USA*, **97**, 9972–9977.
25. Doi, N., Takashima, H., Kinjo, M., Sakata, K., Kawahashi, Y., Oishi, Y., Oyama, R., Miyamoto-Sato, E., Sawasaki, T., Endo, Y. *et al.* (2002) Novel fluorescence labeling and high-throughput assay technologies for *in vitro* analysis of protein interactions. *Genome Res.*, **12**, 487–492.
26. Zhao, H., Giver, L., Shao, Z., Affholter, J.A. and Arnold, F.H. (1998) Molecular evolution by staggered extension process (StEP) *in vitro* recombination. *Nat. Biotechnol.*, **16**, 258–261.
27. Horisawa, K., Tateyama, S., Ishizaka, M., Matsumura, N., Takashima, H., Miyamoto-Sato, E., Doi, N. and Yanagawa, H. (2004) *In vitro* selection of Jun-associated proteins using mRNA display. *Nucleic Acids Res.*, **32**, e169.
28. Miyamoto-Sato, E., Ishizaka, M., Horisawa, K., Tateyama, S., Takashima, H., Fuse, S., Sue, K., Hirai, N., Masuoka, K. and Yanagawa, H. (2005) Cell-free cotranslation and selection using *in vitro* virus for high-throughput analysis of protein–protein interactions and complexes. *Genome Res.*, **15**, 710–717.
29. Stemmer, W.P. (1994) Rapid evolution of a protein *in vitro* by DNA shuffling. *Nature*, **370**, 389–391.
30. Lipovsek, D. and Plückthun, A. (2004) *In vitro* protein evolution by ribosome display and mRNA display. *J. Immunol. Methods*, **290**, 51–67.
31. Blake, D.A., Chakrabarti, P., Khosraviani, M., Hatcher, F.M., Westhoff, C.M., Goebel, P., Wylie, D.E. and Blake, R.C., II (1996) Metal binding properties of a monoclonal antibody directed toward metal–chelate complexes. *J. Biol. Chem.*, **271**, 27677–27685.
32. Kabat, E.A., Wu, T.T., Perry, H.M., Gottesmann, K.S. and Foeller, C. (1991) *Sequences of Proteins of Immunological Interest*. 5th edn. National Institutes of Health Publication No. 91-3242. National Institutes of Health, Bethesda, MD.